Traffic-Load-Adaptive Medium Access Control for Fully Connected Mobile Ad Hoc Networks

Qiang Ye, *Student Member, IEEE*, Weihua Zhuang, *Fellow, IEEE*, Li Li, *Senior Member, IEEE*, and Philip Vigneron

***Abstract*—In this paper, we propose an adaptive medium access control (MAC) solution for a fully connected mobile ad hoc network (MANET), supporting homogeneous best-effort data traffic. The MAC scheme achieves consistently high network performance by adapting to the ever-varying network traffic load. Based on the detection of a current network load condition, nodes can make a switching decision between IEEE 802.11 distributed coordination function (DCF) and dynamic time-division multiple access (D-TDMA), when the network traffic load reaches a threshold, referred to as MAC switching point. The adaptive MAC solution determines the MAC switching point to maximize network performance. Approximate and closed-form performance analytical models for both MAC protocols are established, which facilitate the computation of MAC switching point in a tractable way. Extensive analytical and simulation results demonstrate that the adaptive MAC solution provides consistently maximal network performance in the presence of traffic load dynamics.**

***Index Terms*—Adaptive medium access control (MAC), closed-form expressions, delay, dynamic time-division multiple access (D-TDMA), IEEE 802.11 distributed coordination function (DCF), MAC switching point, mobile ad hoc networks (MANETs), throughput.**

I. Introduction

A typical mobile ad hoc network (MANET) consists of a set of wireless mobile devices (e.g., laptops and smartphones) interconnected and communicating with each other distributedly in either a single-hop mode or a multihop mode [1]–[3]. Due to the infrastructureless characteristic and simplified implementation, MANETs have a great potential to provide cost-effective wireless communication services in areas (e.g., tactical networks and disaster areas) where the conventional communication infrastructures cannot be easily implemented. A well-designed MANET should achieve high network performance and maintain satisfied quality-of-service (QoS) to mobile users. To achieve this goal, proper medium access control (MAC) is required. A MAC protocol is a mechanism to coordinate nodes' access to the wireless medium to transmit their packets. Due to distributed network operation and dynamic traffic load, it is challenging to develop a MAC protocol that can achieve consistently high performance. With no reliance on topology and synchronization information, the carrier sense multiple access with collision avoidance (CSMA/CA)-based IEEE 802.11 DCF contention MAC scheme [4] is mostly widely used in current MANET implementations. However, as the network traffic load increases, the performance of IEEE 802.11 DCF experiences an inevitable degradation, due to an increased amount of control overhead for packet collision resolution. On the other hand, by avoiding packet transmission collisions among nodes, the channelization-based time-division multiple access (TDMA) schemes [5], [6] achieve higher resource utilization than the IEEE 802.11 DCF when the network traffic load is high. However, the distributed time-slot acquisition of TDMA consumes a considerable amount of channel time for local information exchange among neighboring nodes, which makes the channel utilization of TDMA inferior to IEEE 802.11 DCF in a low network traffic load condition [7]. Therefore, there exists a specific network traffic load at which the two MAC protocols have the same performance. We refer to this specific traffic load as the *MAC switching point*. Before the traffic load reaches this point, the performance of IEEE 802.11 DCF is higher than that of TDMA, and after this point, the situation reverses.

Because of the performance trade-off between the contention-based MAC and channelization-based MAC, to make use of the network resources more efficiently, adaptive MAC schemes, combining CSMA/CA (or slotted-Aloha) with TDMA in a hybrid MAC frame pattern, are proposed in literature, which intend to switch between the two MAC frame structures either periodically [8], [9] or via an adaptability to a changing network traffic load [10]–[12]. Generally, the adaptive MAC schemes make the switching between different MAC frame structures based on the estimation of network traffic load through measurements of some microscopic MAC operation parameters (e.g., the number of unused TDMA time slots [10], number of consecutively lost acknowledgments (ACKs) [12], and queue lengths [13]). These microscopic parameters can be effective to reflect the real-time network traffic load condition. However, determining the optimal value of the microscopic MAC switching point, with which the adaptive MAC solutions can achieve maximum performance, is a challenging issue. It is difficult to model the relationship between the microscopic network traffic load indicator and the MAC performance, which is mostly captured by either simulations [10], [12] or experiments [13]. Without an explicit analytical relationship between the MAC performance and the network traffic load indicator, the MAC switching points can only be set empirically, and the

Manuscript received May 23, 2015; revised November 18, 2015; accepted December 21, 2015. Date of publication January 12, 2016; date of current version November 10, 2016. This work was supported by research grants from the Natural Sciences and Engineering Research Council (NSERC) of Canada and from the Communications Research Centre, Ottawa, Canada. The review of this paper was coordinated by Prof. H. Nishiyama.

Q. Ye and W. Zhuang are with the Department of Electrical and Computer Engineering, University of Waterloo, Waterloo, ON N2L 3G1, Canada (e-mail: q6ye@uwaterloo.ca; wzhuang@uwaterloo.ca).

L. Li and P. Vigneron are with the Communications Research Center, Ottawa, ON K2H 8S2, Canada (e-mail: li.li@crc.gc.ca; philip.vigneron@crc.gc.ca).

Color versions of one or more of the figures in this paper are available online at http://ieeexplore.ieee.org.

Digital Object Identifier 10.1109/TVT.2016.2516910

TABLE I
IMPORTANT PARAMETERS AND VARIABLES

Parameter & Variable	Definition
λ	Average packet arrival rate at each node
μ_d	Average packet service rate of each node with IEEE 802.11 DCF
μ_t	Average packet service rate of each node with D-TDMA
ρ	Individual node queue utilization ratio
τ	Packet transmission probability in a backoff slot
$\overline{CW_2}$	Average backoff contention window time
D_T	Average packet delay for IEEE 802.11 DCF
m	Maximum backoff stage
M_L	Retransmission limit
M_m	Number of minislots
N	Total number of nodes in the network
p	Conditional collision probability
T_c	Collision time packets experience during a collision
$\overline{T_c}$	Average collision time encountered before a packet is transmitted
T_m	Minislot duration
T_p	Packet transmission time for D-TDMA
T_{pl}	Duration of packet payload
T_s	Successful packet transmission time for IEEE 802.11 DCF
W	Minimum contention window size
W_{qt}	Packet queueing delay for D-TDMA
W_{st}	Packet access delay for D-TDMA

corresponding switching strategy does not necessarily achieve a maximal performance gain.

In this paper, we develop an adaptive MAC solution for a fully connected MANET in which the MAC switching point between IEEE 802.11 DCF and TDMA is determined based on a theoretical performance comparison of the MAC protocols. Our contribution lies in three aspects. First, for a homogeneous network traffic scenario, whereby all nodes have identical traffic generation statistics, we establish a mathematical relationship between the MAC performance metrics (i.e., throughput and delay) and the macroscopic network traffic load indicator (i.e., the total number of nodes). Second, most existing performance evaluations of either IEEE 802.11 DCF or TDMA rely on numerical methods (Markov chain modeling [4], [14], nonlinear system modeling based on mean value analysis [15]), which do not provide a closed-form expression for performance metrics and are thus computationally complex to conduct a performance comparison between the MAC protocols. To overcome the limitation, we establish a simplified and unified framework, considering both traffic saturation and nonsaturation cases, to make the performance comparison tractable. Approximate and closed-form analytical relations are established between the MAC performance metrics and the total number of nodes in the network for both IEEE 802.11 DCF and TDMA, by using the *least-squares curve-fitting method* and *M/G/1 queueing analysis*, respectively. Third, according to the unified performance analysis framework, an adaptive MAC solution is developed to determine the MAC selection between IEEE 802.11 DCF and TDMA based on the MAC switching point calculation. The MAC switching point is adaptive to traffic load statistics of each node. It is shown that the MAC solution maximizes the network performance in the presence of data traffic load dynamics.

The remainder of this paper is organized as follows. We describe the system model in Section II. Approximate and closed-form performance analytical models for both IEEE 802.11 DCF and TDMA are derived in Section III. The adaptive MAC solution is presented in Section IV, with a focus on calculating the MAC switching point. Analytical and simulation results are provided in Section V to evaluate the performance of the proposed MAC solution. Finally, Section VI concludes this paper.

II. SYSTEM MODEL

A. Network Model

Consider a fully connected MANET [16]–[18] with a single and error-free channel [19], [20]. There is no central controller in the network, and nodes coordinate their transmissions in a distributed way. The destination node for each source node is randomly selected from the remaining nodes. Each mobile node generates best-effort data traffic. The data traffic arrivals at each node are modeled as a Poisson process with an average arrival rate λ packets/s [12], [21], [22]. Packet loss among any pair of source–destination (S–D) nodes results from packet transmission collisions. The total number of nodes in the network is denoted by N, which changes slowly with time (with respect to a packet transmission time), due to user mobility. Some important parameters and variables are listed in Table I.

B. Adaptive MAC Framework

Consider two candidate MAC protocols maintained at each node in the adaptive MAC framework [13], in which a separate mediating MAC entity working on top of the MAC candidates can reconfigure the current MAC layer by switching from one MAC protocol to the other, based on the current network

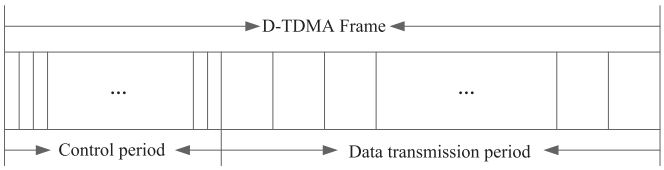

Fig. 1. Frame structure of D-TDMA.

condition (e.g., interference level and the total number of nodes). This adaptation of MAC to the networking environment has a potential to improve the network performance. The contention-based IEEE 802.11 DCF is considered one candidate MAC protocol, which is a standardized and widely adopted MAC scheme based on CSMA/CA. It has a better channel utilization than slotted-Aloha [23], and has high performance at a relatively low contention level. Since we consider a fully connected MANET scenario where no hidden terminal problem exists, the basic access mechanism in IEEE 802.11 DCF is considered.

The channelization-based dynamic TDMA (D-TDMA) scheme [6] is chosen as the other MAC candidate, which is originally used in cellular networks. Time is partitioned to frames of constant duration. Each D-TDMA frame consists of a control period and data packet transmission period. The control period has a number of constant-duration minislots, and data transmission period is composed of a number of equal-length data slots. The duration of each data slot is the time used to transmit one data packet. The number of minislots indicates the maximum number of users the network can support, and the number of data slots equals the current total number of nodes N in the network. The D-TDMA frame structure is shown in Fig. 1. In order to fit the distributed MANET scenario, the minislots in the control period of each D-TDMA frame is used for local information exchange and distributed data slot acquisition of each node. The D-TDMA can support a varying number of nodes in the network and achieve high channel utilization in a high data traffic load.

III. Closed-Form Performance Models for IEEE 802.11 DCF and D-TDMA

Here, a unified performance analysis framework is established for both candidate MAC protocols. We present approximate and closed-form expressions for the relation between performance metrics (i.e., network throughput and packet delay) and the total number of nodes in the network. Both traffic saturation and nonsaturation cases are considered. All the time durations of IEEE 802.11 DCF are normalized to the unit of a backoff time slot in the IEEE 802.11b standard.

A. Closed-Form Performance Models for IEEE 802.11 DCF

In a homogeneous traffic case, because of the throughput fairness property of IEEE 802.11 DCF [24]–[26], the network throughput[1] definition can be made over one renewal cycle[2] of the transmission process. It is defined as the ratio of average payload transmission duration during one renewal cycle over the average length of the cycle [22], given by

$$S=\frac{NT_{\rm pl}}{N\left(T_s+\frac{\overline{T_c}}{2}\right)+\overline{\rm CW_2}+(1-\rho_r)\left[1-(N-1)\rho_r\right]\left(\frac{1}{\lambda}-D_T\right)}. \tag{1}$$

In (1), $T_{\rm pl}$ is the duration of each packet payload; T_s is the successful transmission time of one packet; $\overline{T_c}=(p/1-p)T_c$ is the average collision time encountered by each packet before it is successfully transmitted [20], assuming a large retransmission limit; T_c is the collision time that each packet experiences when a collision occurs; p is the packet collision probability conditioned on which the node attempts a transmission, which is assumed constant and independent of the number of retransmissions; $\overline{\rm CW_2}=(W_0/2)+p(W_1/2)+p^2(W_2/2)+\cdots+p^m(W_m/2)+p^{m+1}(W_m/2)+\cdots+p^{M_L}(W_m/2)$ denotes the average backoff contention window time spent by the tagged node i during the cycle, where $W_j=2^jW(j=0,1,\ldots,m)$ is the backoff contention window size in the jth backoff stage (W is the minimum contention window size); m is the maximum backoff stage; M_L is the retransmission limit; $\rho_r=\lambda/\mu_s=\lambda/N\mu_d$ is the probability with which an incoming packet sees a nonempty queue [22], where μ_s denotes the average service rate of the IEEE 802.11 DCF; μ_d is the average packet service rate seen by an individual node; and D_T is the average packet delay, which is defined as the duration from the instant that a packet arrives at the transmission queue to the instant that the packet is successfully transmitted, averaged over all transmitted packets of each node.

Performance analysis in a traffic saturation case: In a traffic saturation case, (1) can be simplified to represent the saturation throughput S_1, given by

$$S_1=\frac{NT_{\rm pl}}{N\left(T_s+\frac{\overline{T_c}}{2}\right)+\overline{\rm CW_2}} \tag{2}$$

which is a function of the number of nodes N and conditional collision probability p [27]. The collision probability p is correlated with N [15], [28]

$$p=1-(1-\tau)^{N-1} \tag{3}$$

where τ is the packet transmission probability of each node in any backoff time slot given a nonempty queue and can be also expressed as a function of p. Equation (3) captures the collision probability that each packet transmission of the tagged node encounters if at least one of the other $N-1$ nodes transmits in the same backoff time slot. In literature, there are mainly two ways to approximate τ: 1) $\tau=E[M_0]/\overline{\rm CW_2}$ [15], where $E[M_0]=(1-p^{M_L+1})/(1-p)$ is the average number of transmission attempts each node made before the packet is successfully transmitted or discarded due to the retransmission limit M_L; and 2) $\tau=1/\overline{\rm CW_1}$ [28], where $\overline{\rm CW_1}=((1-p-p(2p)^m)/(1-2p))(W/2)$ is the average backoff contention window size between two consecutive packet transmission attempts of the tagged node. Both approximations of τ can be substituted into (3) for solving p with certain N.

[1]The throughput in this paper is normalized by the channel rate.

[2]The transmission attempt process of each node can be regarded as a regenerative process, with the renewal cycle being the time between two successfully transmitted packets of the node [22].

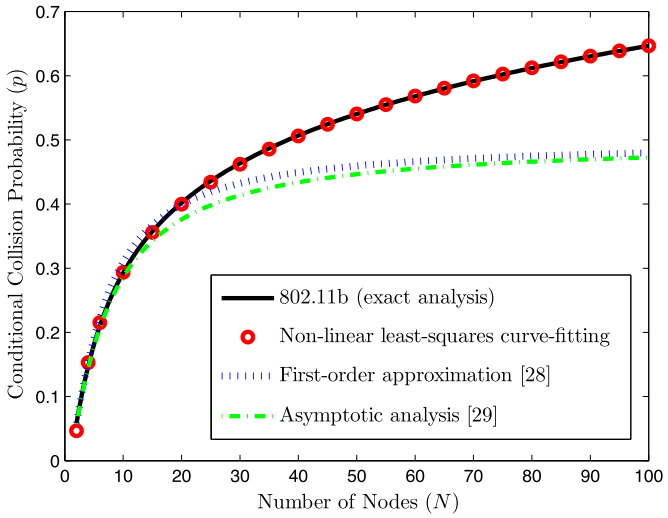

Fig. 2. Least-squares curve-fitting between p and N.

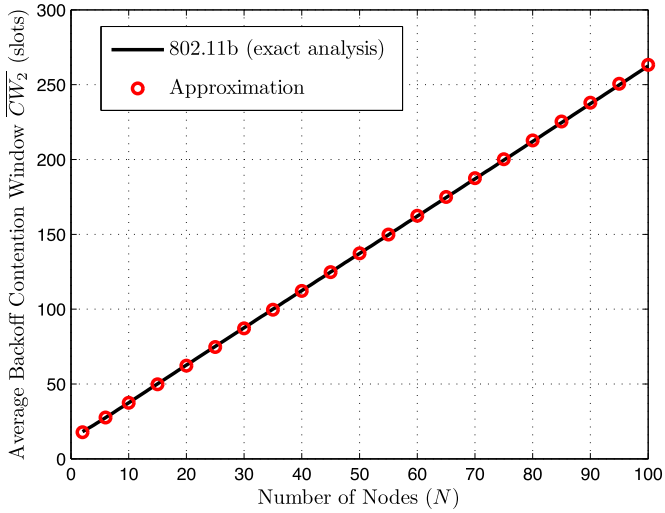

Fig. 3. Approximation of average backoff contention window $\overline{\mathrm{CW}_2}$.

Since variables p and N are correlated in (3), i.e., a high-degree nonlinear equation whose computational complexity gets higher with an increase in degree N, the saturation throughput S_1, as a function of both variables, can be evaluated only by solving (3) numerically [22], [29]. Thus, the throughput model of (2) and (3) is a nonlinear system that does not provide a closed-form expression for S_1. Based on this numerical performance model, it is computationally complex to conduct a performance comparison between IEEE 802.11 DCF and the other MAC candidate. Therefore, we aim to make some approximation on (3) to get an explicit closed-form relation between p and N, which can be directly substituted into (2) to simplify S_1 as a closed-form function of only N.

Some approximations are available in literature to simplify (3) (e.g., first-order approximation [28], asymptotic analysis [29]). However, as shown in Fig. 2, the accuracy of these approximations drops when N becomes larger. In [22], the exact relationship between p and N is depicted by solving (3) for p over a wide range of N using numerical techniques. It is stated that p increases both monotonically and logarithmically with N, provided that m, M_L, and W are specified based on the IEEE 802.11b standard. Thus, to get a more accurate closed-form function between p and N, we use a *nonlinear least-squares curve-fitting method* to fit the relation between both variables

$$\min_{\mathbf{a}=(a_1,a_2)} \|a_1 + a_2 \ln(\mathbf{N}) - \mathbf{P}\|_2^2 \text{ subject to } a_2 \geq 0 \quad (4)$$

where vectors $\mathbf{N} = \{n | n \in \mathbb{Z}^+\}$ and $\mathbf{P} = \{p_n | n \in \mathbb{Z}^+\}$ are data sets of N and p, respectively, satisfying (3), and $\mathbf{a} = (a_1, a_2)$ is the vector of the fitting coefficients. In (4), the bounded constraint makes the optimization problem converge fast to an optimal solution [30].

Proposition 1: Global optimal fitting coefficients in (4) exist since the logarithmic nonlinear least-squares curve-fitting is a convex optimization problem.

The proof of Proposition 1 is given in Appendix A. The logarithmic curve-fitting relation obtained between p and N is

$$p \approx a_1 + a_2 \ln(N) = -0.0596 + 0.1534 \ln(N). \quad (5)$$

Fig. 2 shows that the closed-form logarithmic fitting function is much more accurate to approximate p, over a wide range of N, than the existing approximations in [28] and [29]. Since the fitting function explicitly expresses p as a function of N, S_1 can be simplified as a closed-form function of only N, by substituting (5) into (2). However, since the average backoff contention window $\overline{\mathrm{CW}_2}$ is a high-degree function of p, the approximate expression of S_1 is still complicated. The expression of $\overline{\mathrm{CW}_2}$ can be approximated by an exponential function of p because the Taylor expansion of an exponential function has a mathematical form similar to the expression of $\overline{\mathrm{CW}_2}$, i.e.,

$$\begin{aligned}\overline{\mathrm{CW}_2} &= \frac{W_0}{2} + \frac{W_1}{2}p + \frac{W_2}{2}p^2 + \cdots + \frac{W_m}{2}p^m + \frac{W_m}{2}p^{m+1} \\ &\quad + \cdots + \frac{W_m}{2}p^{M_L} \\ &\approx b_1 + b_2 \exp(b_3 p) \\ &= (b_1 + b_2) + b_2 b_3 p + b_2 \frac{b_3^2}{2!}p^2 + b_2 \frac{b_3^3}{3!}p^3 + \cdots \end{aligned} \quad (6)$$

where $(b_1, b_2, b_3) = (12.9590, 3.5405, 6.5834)$ are the coefficients of the exponential function obtained through the nonlinear least-squares curve-fitting method. Then, by substituting (5) into (6), $\overline{\mathrm{CW}_2}$ can be further approximated by a closed-form function of N

$$\begin{aligned}\overline{\mathrm{CW}_2} &\approx b_1 + b_2 \exp\left[b_3 \left(a_1 + a_2 \ln(N)\right)\right] \\ &= b_1 + b_2 \exp(b_3 a_1) \exp\left[b_3 a_2 \ln(N)\right]. \end{aligned} \quad (7)$$

Fig. 3 shows that $\overline{\mathrm{CW}_2}$ has a nearly linear relation with N since $b_3 a_2 \approx 1$ in (7).

By substituting (5) and (7) into (2), we obtain a simplified and closed-form expression of S_1, as a function of N, given by (8), shown at the bottom of the next page, where T_s, T_{pl}, and T_c are known parameters specified in the IEEE 802.11b standard. Fig. 4 demonstrates that the simplified analytical function $S_1(N)$ is an accurate approximation of the numerical performance model [22], [27] represented by the nonlinear system of (2) and (3).

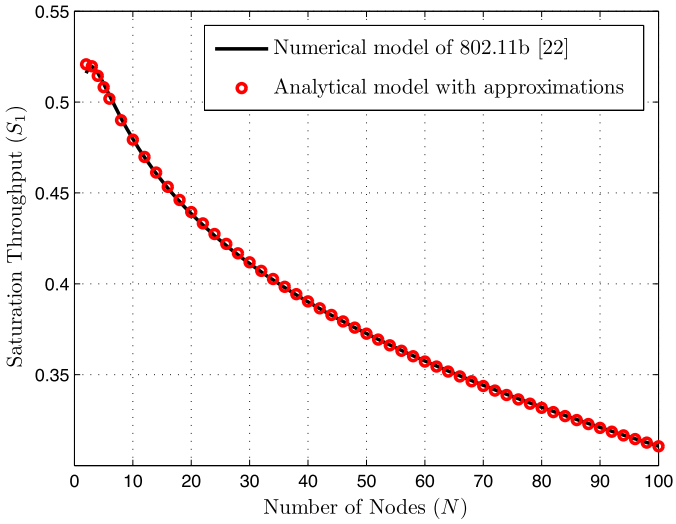

Fig. 4. Saturation throughput S_1 and its approximation.

In the traffic saturation case, the average packet access delay (average packet service time) D_1 is defined as the duration from the instant that the packet becomes the head of the transmission queue to the instant that the packet is successfully transmitted, averaged over all transmitted packets of each node. Since D_1 is the denominator of S_1 [22], it can also be approximated by a closed-form analytical function of N, given by (9), shown at the bottom of the page.

Performance analysis in a traffic nonsaturation case: When the network is nonsaturated, the average packet arrival rate λ of each node should not exceed its service capacity share μ_d. The packet queue at each node possibly becomes empty upon successful transmission of the previous packet. The derivation of the packet transmission probability should account for the fact that a node attempts a transmission only when it has packets to transmit. Thus, (3) should be revised to

$$p = 1 - (1 - \rho \cdot \tau)^{N-1} \tag{10}$$

where $\rho = \lambda/\mu_d$ is the queue utilization ratio of an individual node, and $\rho\tau$ is the packet transmission probability of each node.

Due to its fairness property, the IEEE 802.11 system can be viewed as a server that schedules its resources to the contending nodes in a round robin manner [22]. In each scheduling cycle, every node (out of N nodes) can occupy an average fraction of $1/N$ system bandwidth to successfully transmit one packet. This service system is called processor sharing (PS) system. Thus, the IEEE 802.11 DCF can be modeled as an M/G/1/PS system with cumulative arrival rate $\lambda_s = N\lambda$ and service rate $\mu_s = N\mu_d$. According to [22], this M/G/1/PS system has the same access delay and queueing delay as the M/M/1 queueing system with equivalent average arrival rate λ_s and service rate μ_s. Thus, the average packet delay in the M/G/1/PS system is a summation of average packet access delay and average packet queueing delay (i.e., the duration from the instant that the packet arrives at the transmission queue to the instant that the packet becomes the queue head averaged over all transmitted packets of each node), given by

$$D_T = \frac{1}{\mu_s - \lambda_s} \tag{11}$$

where $\mu_s = [T_s + (\overline{T_c}/2) + (\overline{\mathrm{CW}_2}/N)]^{-1}$ [22].

Similar to the traffic saturation case, since p and N are correlated as in the high-degree nonlinear relation, (10) and (11) form a nonlinear system with two variables p and N that can be solved using numerical techniques [15], [22]. To get a simplified and closed-form performance expression as a function of N, one approach is to obtain an explicit relation between p and N. A first-order approximation of (10) and linearizing the transmission probability as $\tau \approx (2W/(W+1)^2)(1-p)$ [31] can be applied to simplify (10) to a quadratic equation of p, given by

$$\begin{aligned} p &\approx (N-1)\lambda \left[N\left(T_s + \frac{\overline{T_c}}{2}\right) + \overline{\mathrm{CW}_2} \right] \tau \\ &\approx (N-1)\lambda \left[\frac{2WNT_s}{(W+1)^2}(1-p) \right. \\ &\qquad \left. + \frac{NT_cW}{(W+1)^2}p + \frac{1}{1-p} \right] (\tau, p \ll 1). \end{aligned} \tag{12}$$

Then, with packet arrival rate λ, a closed-form relation between p and N can be established by solving the quadratic equation of p. However, this first-order approximation is accurate only when p and τ are much less than one for a small value of N, as shown in Fig. 5(a) and (b). To have a more accurate approximation, we solve (10) for p over a wide range of N under the condition that all nodes are traffic nonsaturated. It is found out that, with different values of λ, linearizing p as a function of N better characterizes the relation between p and N. Thus, a *linear least-squares curve-fitting method* is used to

$$S_1(N) = \frac{NT_{\mathrm{pl}}}{NT_s + \frac{N}{2}\frac{a_1 + a_2\ln(N)}{1-[a_1+a_2\ln(N)]}T_c + b_1 + b_2\exp(b_3a_1)\exp\left[b_3a_2\ln(N)\right]} \tag{8}$$

$$D_1(N) = NT_s + \frac{N}{2}\frac{a_1 + a_2\ln(N)}{1-[a_1+a_2\ln(N)]}T_c + b_1 + b_2\exp(b_3a_1)\exp\left[b_3a_2\ln(N)\right] \tag{9}$$

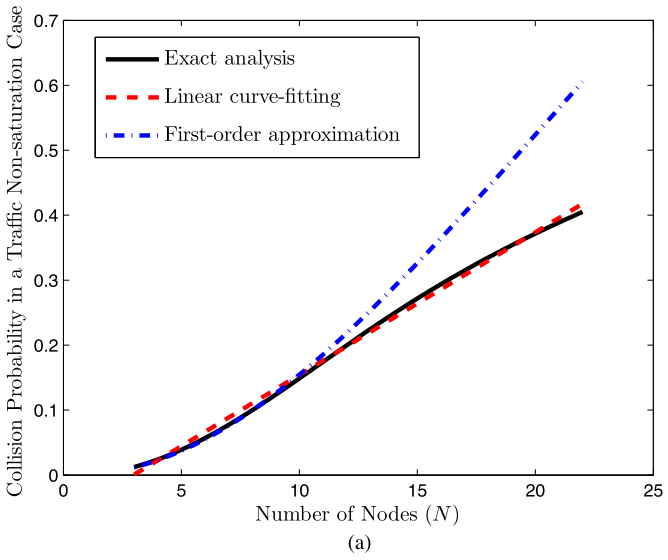

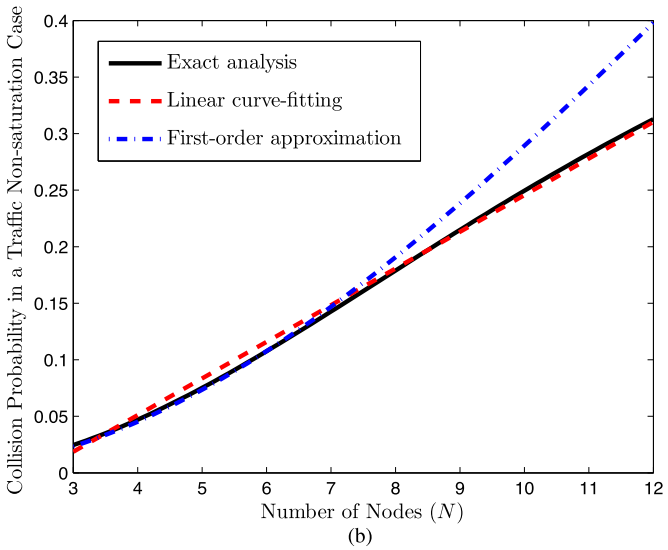

Fig. 5. Approximations for collision probability in a traffic nonsaturation case. (a) $\lambda = 25$ packets/s. (b) $\lambda = 50$ packets/s.

find a closed-form linear function between p and N, which is denoted by $p(N, \lambda)$ as an approximation of (10), shown in Fig. 5(a) and (b). Substituting $p(N, \lambda)$ into $\overline{T_c}$ in (1) yields a closed-form function $\overline{T_c}(N, \lambda) = (p(N, \lambda)/(1 - p(N, \lambda)))T_c$.

Since p shows a near linear relation with N for different values of λ and $\overline{\text{CW}_2}$ is approximately an exponential function of p in (6), $\overline{\text{CW}_2}$ can be approximately represented as an exponential function of N, denoted by $\overline{\text{CW}_2}(N, \lambda)$. Therefore, a closed-form expression for average packet delay D_T in terms of N is obtained as

$$D_2(N, \lambda) = \frac{1}{\mu_s(N, \lambda) - N\lambda} \tag{13}$$

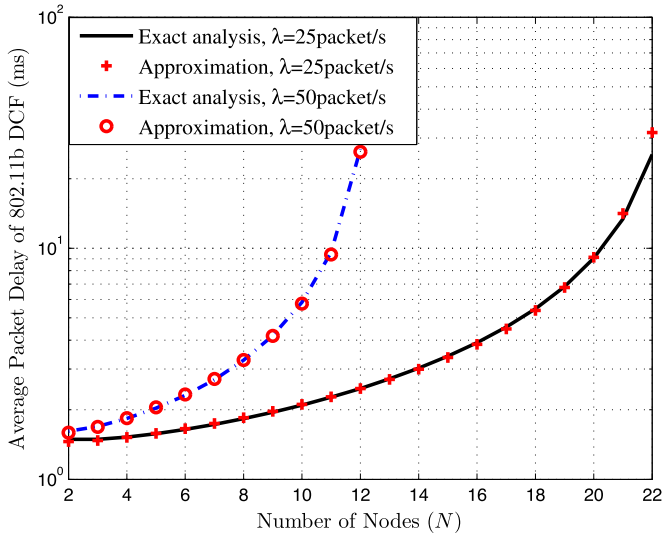

Fig. 6. Average packet delay of IEEE 802.11 DCF and its approximation for $\lambda = 25$ and 50 packets/s, respectively.

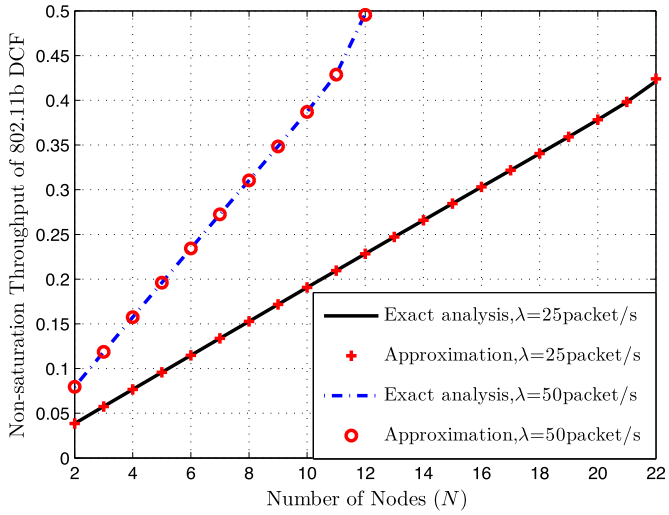

Fig. 7. Nonsaturation throughput of IEEE 802.11 DCF and its approximation for $\lambda = 25$ and 50 packets/s, respectively.

where $\mu_s(N, \lambda) = [T_s + (\overline{T_c(N, \lambda)}/2) + (\overline{\text{CW}_2(N, \lambda)}/N)]^{-1}$ is a closed-form expression for μ_s.

Similarly, the nonsaturated network throughput, with the general form in (1), has the approximate and closed-form expression given in (14), shown at the bottom of the page. Figs. 6 and 7 show the exact values of average packet delay and nonsaturation throughput as well as their accurate approximations over a wide range of N. It can be seen that, for λ equal to 25 and 50 packets/s, the traffic of each node enters the saturation state when N increases to the values greater than 22 and 12, respectively.

$$S_2(N, \lambda) = \frac{NT_{\text{pl}}}{N\left(T_s + \frac{\overline{T_c(N,\lambda)}}{2}\right) + \overline{\text{CW}_2(N, \lambda)} + \left[1 - \frac{\lambda}{\mu_s(N,\lambda)}\right]\left[1 - (N-1)\frac{\lambda}{\mu_s(N,\lambda)}\right]\left[\frac{1}{\lambda} - D_2(N, \lambda)\right]} \tag{14}$$

B. Closed-Form Performance Models for D-TDMA

Performance analysis in a traffic saturation case: When the network is saturated, we can obtain closed-form expressions of throughput and delay as a function of N. Since N in general varies slowly with respect to the frame duration, the network saturation throughput S_3 is approximately given by

$$S_3(N) = \frac{NT_{\rm pl}}{NT_p + M_m T_m} \tag{15}$$

where $T_{\rm pl}$ is the duration of payload information of each data packet, T_p is the data packet duration including headers, M_m denotes the number of minislots in the control period of each D-TDMA frame, and T_m is the duration of each minislot.

Moreover, the average packet access delay of D-TDMA, denoted by D_3, can be expressed as

$$D_3(N) = NT_p + M_m T_m. \tag{16}$$

Performance analysis in a traffic nonsaturation case: In order to simplify the analysis of packet access delay and queueing delay, denoted by $W_{\rm st}$ and $W_{\rm qt}$, respectively, we assume that nodes release their data slots and randomly acquire new ones in the next frame, after transmitting a packet in the data transmission period of current frame [32]. This assumption guarantees that the service times of successive packets are independent identically distributed (i.i.d.) random variables. Based on this assumption, the queue of each node in the traffic nonsaturation case can be modeled as an M/G/1 queueing system [32], with an average service rate denoted by μ_t packets/s. We derive the distribution of packet service time $W_{\rm st}$ to calculate the average packet access delay $E[W_{\rm st}]$ in the M/G/1 system. Then, the P-K formula [33] can be used to calculate the average packet queueing delay, $E[W_{\rm qt}]$, for each M/G/1 queue, based on the second moment of $W_{\rm st}$, denoted by $E[W_{\rm st}^2]$. As a result, the average packet delay D_4, which is the summation of $E[W_{\rm st}]$ and $E[W_{\rm qt}]$ (see Appendix B for the derivation of $E[W_{\rm st}]$ and $E[W_{\rm qt}]$), is given by

$$D_4 = E[W_{\rm st}] + \frac{\lambda E\left[W_{\rm st}^2\right]}{2\left[1 - \lambda E[W_{\rm st}]\right]}. \tag{17}$$

Since $E[W_{\rm st}]$ and $E[W_{\rm st}^2]$ are both functions of N, D_4 is also a closed-form function of N, denoted by $D_4(N, \lambda)$.

As to the nonsaturation throughput analysis, the probability that the queue of a tagged node is nonempty at the start of its designated time slot, denoted by $P_{\rm qn}$, is given by

$$P_{\rm qn} = \frac{\lambda}{\mu_t} \tag{18}$$

where $\mu_t = 1/E[W_{\rm st}] = (2 - \lambda(M + N - 1)T_p)/(M + N + 1)T_p$, M denotes the duration of each control period normalized to the unit of one D-TDMA data slot duration, according to the delay analysis in Appendix B.

Thus, we use random variable X to denote the number of nodes with nonempty queues at the start of their designated time slots during the time of one frame. The probability mass function (PMF) and the average of random variable X are given by [14]

$$P\{X = k\} = \binom{N}{k}\left(\frac{\lambda}{\mu_t}\right)^k\left(1 - \frac{\lambda}{\mu_t}\right)^{N-k}, \quad k = 0, 1, \ldots, N \tag{19}$$

$$E[X] = N \cdot \frac{\lambda}{\mu_t}. \tag{20}$$

Hence, the network nonsaturation throughput S_4 can be approximated as a function of N

$$S_4(N, \lambda) = \frac{N\lambda T_{\rm pl}}{\mu_t(NT_p + M_m T_m)}. \tag{21}$$

In summary, we derive simplified and closed-form throughput and delay expressions $S_1(N)$, $S_2(N, \lambda)$, $D_1(N)$, $D_2(N, \lambda)$ for the IEEE 802.11 DCF, and $S_3(N)$, $S_4(N, \lambda)$, $D_3(N)$, $D_4(N, \lambda)$ for D-TDMA, respectively, for both traffic saturation and nonsaturation cases. The expressions can greatly simplify the MAC switching point calculation.

IV. Adaptive MAC Solution

Here, we present a MAC protocol that adapts to the changing traffic load in the MANET. The key element is to determine the MAC switching point with which an appropriate candidate MAC protocol is selected to achieve better performance in terms of throughput and delay at each specific network traffic load condition. Based on the closed-form expressions derived in Section III, we establish a unified performance analysis framework to evaluate the throughput and delay over a wide range of N for both nonsaturated and saturated network traffic conditions. Taking throughput evaluation as an example, in this framework, when N is small, the network is nonsaturated and the throughput is represented analytically by $S_2(N, \lambda)$ and $S_4(N, \lambda)$ for IEEE 802.11 DCF and D-TDMA, respectively. With an increase in N, packet service rates μ_d and μ_t of each node with both MAC protocols decrease consistently, making the queue utilization ratio of each node approach to one. After a specific network load saturation point in terms of N, e.g., N_1 (N_2), where the arrival rate λ equals the service rate μ_d (μ_t), the network operating in IEEE 802.11 DCF (D-TDMA) enters the traffic saturation state. Thus, $S_1(N)$ and $S_3(N)$ are used to represent the network saturation throughput for each MAC candidate, respectively.

With this unified framework, performance comparison between the MAC candidates, with respect to N, can be conducted to calculate the MAC switching point. However, since IEEE 802.11 DCF and D-TDMA have different service capacity, the saturation points N_1 and N_2 are in general different, depending on λ. Therefore, the MAC switching point can be a specific network traffic load point, where the network with either IEEE 802.11 DCF or D-TDMA has four possible traffic state combinations: 1) The network is in the traffic saturation state with both MAC candidates; 2) the network is in the traffic nonsaturation state with both MAC candidates; 3) the network is traffic saturated with IEEE 802.11 DCF and traffic nonsaturated with D-TDMA; and 4) the network is traffic nonsaturated with IEEE 802.11 DCF and traffic saturated with D-TDMA. The established unified closed-form expressions facilitate

performance comparison and the calculation of MAC switching point denoted by N_s (in terms of the number of nodes), for the four possible cases. The MAC switching point may vary, due to variations of λ at each node, in the homogeneous network traffic scenario. Algorithm 1 presents the detail steps of determining N_s. As an example, we illustrate step by step the switching point calculation for $\lambda = 25$ and 50 packets/s, respectively, based on network throughput comparison. Then, the complete MAC switching point calculation algorithm is provided, considering all the possible cases.

Algorithm 1: MAC switching point calculation algorithm

Input : The saturation points, N_1 and N_2, for IEEE 802.11 DCF and D-TDMA.

Output: The MAC switching point N_s.

```
if N1 < N2 then
    if S1(N1) > S4(N1, λ) then
        if S1(N2) < S3(N2) then
            Ns ← solving S1(N) = S4(N, λ);
        else
            Ns ← solving S1(N) = S3(N);
        end
    else if S1(N1) < S4(N1, λ) then
        Ns ← solving S2(N, λ) = S4(N, λ);
    else
        Ns ← N1;
    end
else if N1 > N2 then
    if S3(N2) > S2(N2, λ) then
        Ns ← solving S2(N, λ) = S4(N, λ);
    else if S3(N2) < S2(N2, λ) then
        if S3(N1) > S1(N1) then
            Ns ← solving S2(N, λ) = S3(N);
        else
            Ns ← solving S1(N) = S3(N);
        end
    else
        Ns ← N2;
    end
else
    if S1(N1) ≥ S3(N1) then
        Ns ← solving S1(N) = S3(N);
    else
        Ns ← solving S2(N, λ) = S4(N, λ);
    end
end
```

1) $\lambda = 25$ packets/s:

Step 1. Compare the saturation points N_1 and N_2 for both MAC candidates $N_1 < N_2$;

Step 2. Compare the throughput of both MAC candidates at N_1, $S_1(N_1) > S_4(N_1, \lambda)$;

Step 3. Compare the throughput of both MAC candidates at N_2, $S_3(N_2) > S_1(N_2)$;

Step 4. The MAC switching point is calculated by solving the equation $S_1(N) = S_4(N, \lambda)$, where the network has saturated traffic operating in IEEE 802.11 DCF and nonsaturated traffic operating in D-TDMA.

2) $\lambda = 50$ packets/s:

Step 1. Compare the saturation points N_1 and N_2 for both MAC candidates, $N_1 = N_2 = N^*$;

Step 2. Compare the throughput of both MAC candidates at N^*, $S_1(N^*) = S_3(N^*)$;

Step 3. The MAC switching point is obtained as $N_s = N^*$, where the network has saturated traffic operating in either candidate MAC protocol.

The MAC switching point can also be determined based on comparison of average packet delay between the MAC candidates, which is expected to generate similar results since a higher throughput corresponds to a lower packet delay. In theory, the average packet delay can be evaluated only when the packet arrival rate is less than the service rate, where the network traffic is in the nonsaturation state. Otherwise, the packet delay will theoretically approach infinity. Therefore, when the MAC switching point locates at an N value where the network is in a traffic saturation state with either candidate MAC protocol, the average packet access delay $D_1(N)$ and $D_3(N)$ can be used to calculate the switching point.

Due to node mobility, the number of nodes N may fluctuate around the switching point when nodes move relatively fast, resulting in undesired frequent MAC switching (taking account of switching cost). In order to benefit from the MAC switching, the performance gain should be higher than the switching cost. Therefore, the MAC switching point can be replaced by a switching interval. The MAC switching is triggered only if the number of nodes N varies beyond the switching interval. The length of the switching interval depends on the performance gain and switching cost.

V. Numerical Results

Here, we present analytical and simulation results for performance evaluation of both MAC candidates and the MAC switching point. The simulation results are used to demonstrate the accuracy of the MAC switching point calculation based on the closed-form expressions in Section III. With an error-free wireless channel in the system, we use the network simulator, OMNeT++ [34], [35], to simulate the IEEE 802.11b DCF and the D-TDMA. In the simulation, a fully connected network over a 50 m $\times$ 50 m square coverage area is deployed, where nodes are randomly scattered. Traffic arrivals for each node are realized as a Poisson process with λ being 25 and 50 packets/s, respectively, for the nonsaturated traffic case, and with λ set as 500 packets/s for the saturated traffic case. Each simulation point provides the average value of the corresponding performance metrics (i.e., throughput and delay). We also plot the 95% confidence intervals for each simulation result. Note that some confidence intervals are very small in the figures. Other main simulation parameters are summarized in Table II.

A. Traffic Saturation Case

First, the saturation throughputs of both MAC candidates are plotted in Fig. 8(a)–(c), for $M_m = 15$, 25, and 35, respectively. It is observed that the analytical and simulation results

TABLE II
SIMULATION PARAMETERS USED IN IEEE 802.11B [36] AND D-TDMA

Parameters \ MAC schemes	IEEE 802.11b	D-TDMA
Channel capacity	11Mbps	11Mbps
Basic rate	1Mbps	1Mbps
Backoff slot time	20 μs	—
Minimum contention window size (W)	32	—
Maximum contention window size (W_m)	1024	—
Retransmission limit (M_L)	7	—
Guard time (GT) [6]	—	1 μs
PLCP & Preamble	192 μs	192 μs
MAC header duration	24.7 μs	24.7 μs
Packet payload duration (T_{pl})	$\frac{8184}{11}$ μs	$\frac{8184}{11}$ μs
Short interframe space (SIFS)	10 μs	—
ACK	10.2 μs	—
Distributed interframe space (DIFS)	50 μs	—
Minislot duration (T_m)	—	219.4 μs
Network size upper limit (M_m)	15/25/35 nodes	15/25/35 nodes
Queue length	10000 packets	10000 packets

closely agree with each other. As M_m increases, the saturation throughput of D-TDMA decreases since the length of the control period in each D-TDMA frame increases, which reduces the channel utilization. The two MAC candidates have near opposite throughput variation trends as the network traffic load increases. For IEEE 802.11 DCF, the saturation throughput decreases with an increase in the traffic load. On the other hand, the saturation throughput of D-TDMA experiences a consistent rise when the number of nodes increases. Therefore, the two throughput curves intersect at a specific network traffic load value, e.g., $N = 12.5$ when $M_m = 35$. Before this value, IEEE 802.11 DCF outperforms D-TDMA and, after this value, the D-TDMA performs better. Thus, the MAC switching point is the first integer number of nodes after the intersection, i.e., $N_s = 13$.

The average packet access delay of both MAC candidates in a traffic saturation case are plotted in Fig. 9(a)–(c), for $M_m = 15, 25, 35$, respectively. It is observed that the MAC switching point is almost the same as that based on the saturation throughput.

B. Traffic Nonsaturation Case

Fig. 10(a) and (b) show how the network throughput changes with the number of nodes for both MAC schemes at $\lambda = 25$ and 50 packets/s, respectively. Again, the analytical results closely match the simulation results. In the simulation, we start from $N = 2$, where each node has a nonsaturated traffic for both MAC candidates and gradually increase the N value to $N = 35$. As N increases, the service rate for each node decreases, and the traffic at each node becomes saturated after N increases to a certain value. For IEEE 802.11 DCF, the saturation point locates at $N_1 = 23$ and 13 for λ equal to 25 packets/s and 50 packets/s, respectively. On the other hand, the corresponding saturation point of D-TDMA is $N_2 = 33$ and 13, respectively. When the traffic load is low, the nonsaturation network throughput of IEEE 802.11 DCF is greater than that of D-TDMA; therefore, nodes should choose IEEE 802.11 DCF as the initial MAC scheme. For $\lambda = 25$ packets/s, the MAC switching point is $N_s = 26$, where nodes with IEEE 802.11 DCF are traffic saturated. For $\lambda = 50$ packets/s, the switching point appears at $N_s = 13$, from which nodes with either MAC scheme have saturated traffic.

Fig. 11(a) and (b) shows the average packet delay for both MAC candidates in a traffic nonsaturation case with $\lambda = 25$ and 50 packets/s, respectively, for N varying from 2 to the largest integer within traffic nonsaturation load region. We can see that the analytical results closely match the simulation results and the confidence intervals are very small. For $\lambda = 25$ packets/s, the two delay curves are expected to intersect at the network load point where IEEE 802.11 DCF becomes traffic saturated and D-TDMA is still traffic nonsaturated. Thus, the MAC switching point exists as the saturation point of IEEE 802.11 DCF, which is denoted $N_s = 23$. For $\lambda = 50$ packets/s, the two delay curves do not intersect in the traffic nonsaturation state. Thus, the MAC switching point is expected to exist at a traffic saturated load point greater than $N = 12$, which can be obtained analytically as $N_s = 13$ based on comparison of average packet access delay for both MAC candidates, shown in Fig. 9(c). The MAC switching point based on packet delay comparison is almost the same as that based on throughput comparison.

VI. CONCLUSION

In this paper, we consider adaptive MAC between IEEE 802.11 and D-TDMA to maximize network performance over traffic load variations. We propose a novel analytical model to calculate the MAC switching point for a fully connected MANET with homogeneous best-effort data traffic support.

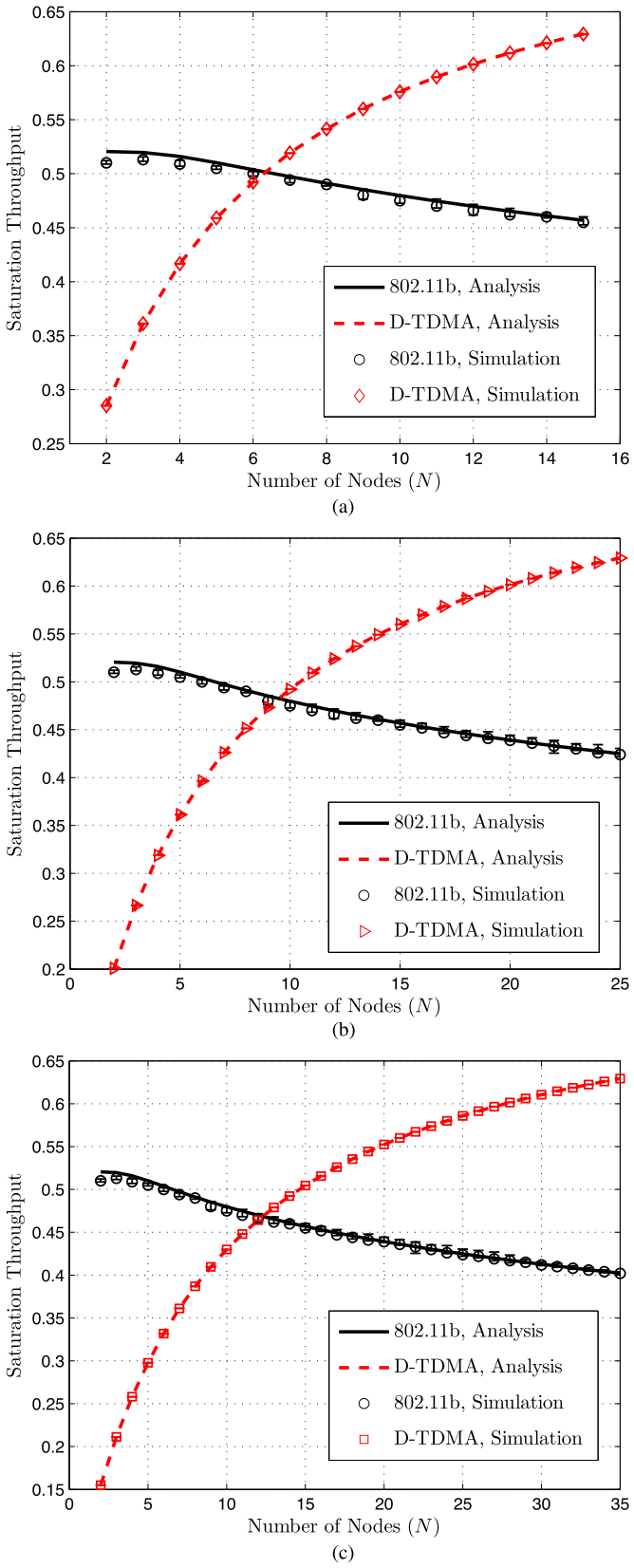

Fig. 8. Saturation throughput of both MAC schemes. (a) $M_m = 15$. (b) $M_m = 25$. (c) $M_m = 35$.

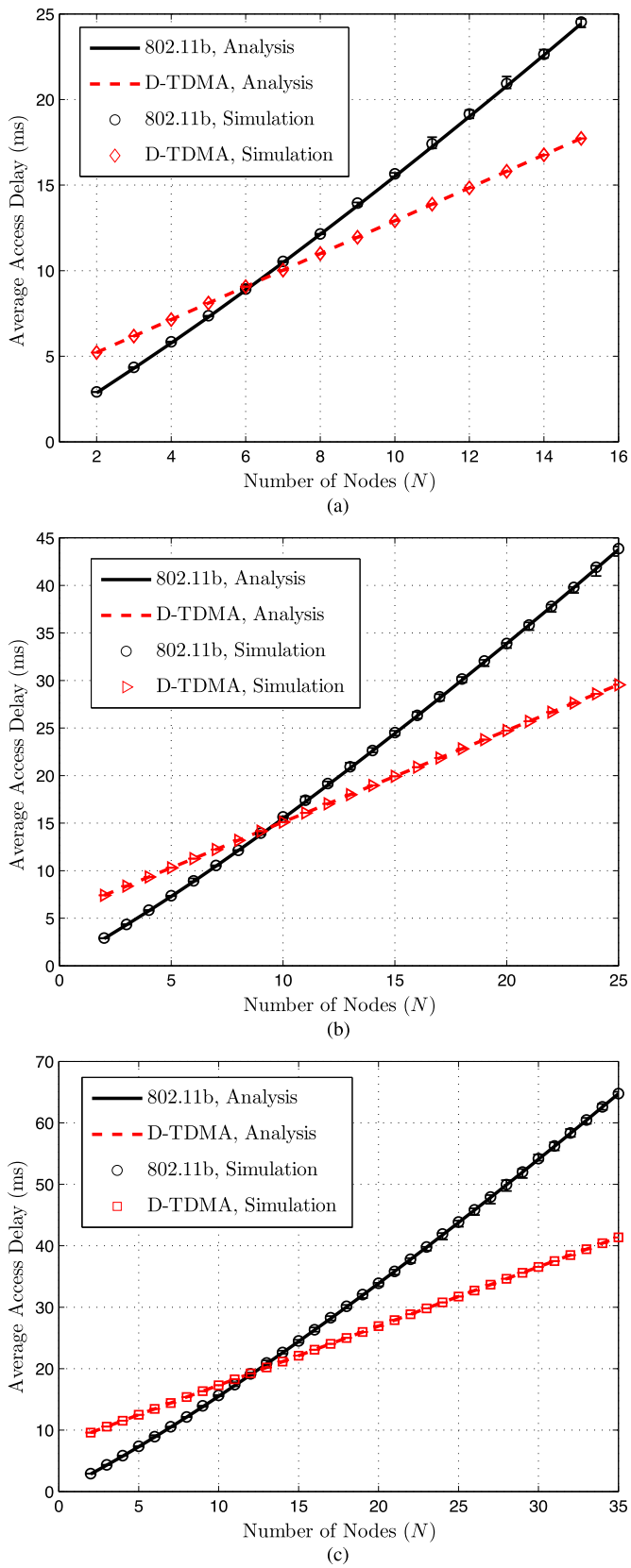

Fig. 9. Average packet access delay of both MAC schemes. (a) $M_m = 15$. (b) $M_m = 25$. (c) $M_m = 35$.

Based on the switching point, nodes can make a switching decision between IEEE 802.11 DCF and D-TDMA in a distributed manner when the network traffic load varies. Approximate and closed-form expressions for network performance in terms of the total number of nodes in the network are presented for both MAC candidates to facilitate the calculation of MAC switching

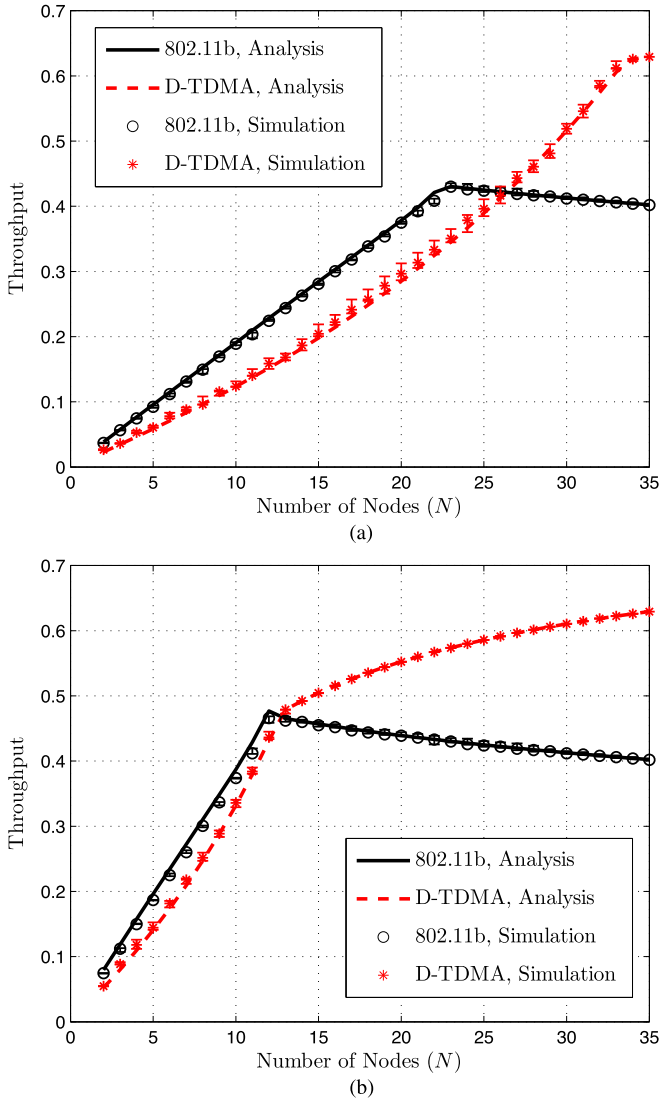

Fig. 10. Network throughput versus the number of nodes. (a) $\lambda =$ 25 packets/s. (b) $\lambda = 50$ packets/s.

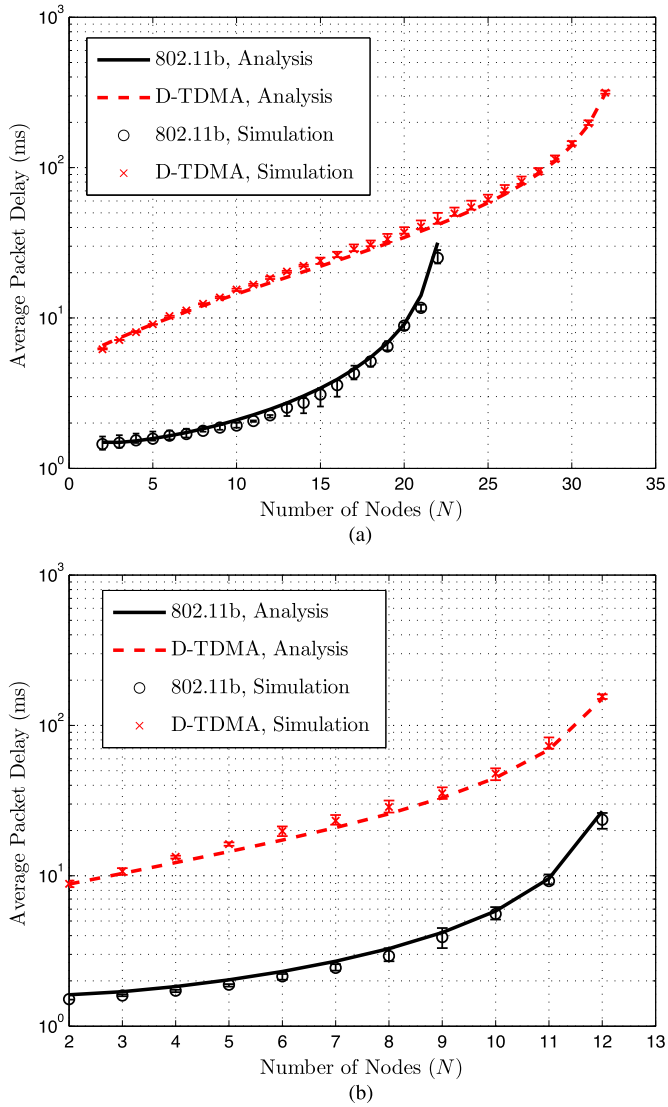

Fig. 11. Average packet delay versus the number of nodes. (a) $\lambda =$ 25 packets/s. (b) $\lambda = 50$ packets/s.

point. Analytical and simulation results demonstrate the high accuracy of the proposed analytical model in determining the MAC switching point, in both saturated and unsaturated traffic load conditions. For our future work, we intend to extend the adaptive MAC solution to support heterogeneous services (i.e., both real-time voice and non-real-time best-effort data applications) in a fully connected MANET.

Appendix A
Proof of Proposition 1

The objective function of the logarithmic nonlinear least-squares curve-fitting problem can be written as

$$\|a_1 + a_2 \ln(\mathbf{N}) - \mathbf{P}\|_2^2 = \sum_{n=2}^{N} (a_1 + a_2 \ \ln(n) - p_n)^2 = \sum_{n=2}^{N} f_n^2(\mathbf{a}). \quad (22)$$

Then, $\forall\, \mathbf{a} \in \mathbf{dom}\ f_n$, we calculate the Hessian matrix of $f_n^2(\mathbf{a})$ as follows:

$$\mathbf{H}\left(f_n^2(\mathbf{a})\right) = \begin{bmatrix} \frac{\partial f_n^2(\mathbf{a})}{\partial a_1^2} & \frac{\partial f_n^2(\mathbf{a})}{\partial a_1 \partial a_2} \\ \frac{\partial f_n^2(\mathbf{a})}{\partial a_2 \partial a_1} & \frac{\partial f_n^2(\mathbf{a})}{\partial a_2^2} \end{bmatrix} = \begin{bmatrix} 2 & 2\ln(n) \\ 2\ln(n) & 2\ln^2(n) \end{bmatrix}. \quad (23)$$

The eigenvalues of the Hessian matrix can be derived by solving the eigenfunction of $\mathbf{H}(f_n^2)$

$$\mathbf{det}\left(\lambda\, \mathbf{I} - \mathbf{H}\left(f_n^2\right)\right) = \begin{vmatrix} \lambda - 2 & -2\ln(n) \\ -2\ln(n) & \lambda - 2\ln^2(n) \end{vmatrix} = 0$$

$$\Longrightarrow \lambda_1 = 0, \lambda_2 = 2 + 2\ln^2(n). \quad (24)$$

Because both eigenvalues of $\mathbf{H}(f_n^2)$ are nonnegative, the Hessian matrix $\mathbf{H}(f_n^2)$ is semi-definite. On the other hand, since $\mathbf{dom}\ f_n = \{(a_1, a_2) \mid a_2 \geq 0\}$ is a convex set, $f_n^2(\mathbf{a})$ is a convex function for all $\mathbf{a} \in \mathbf{dom}\ f_n$.

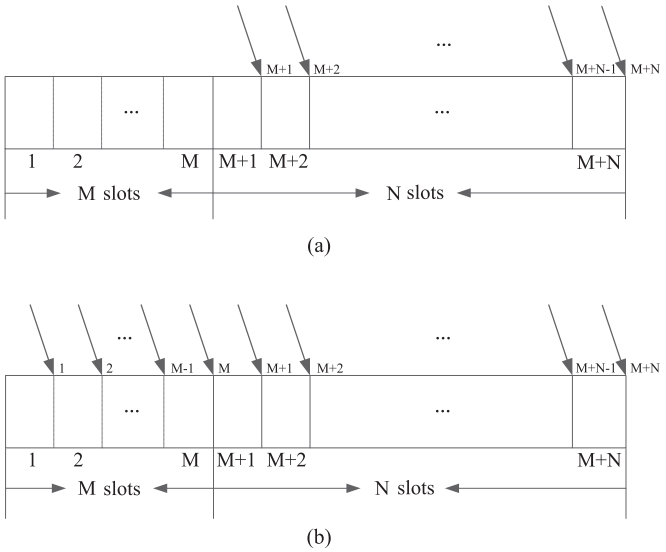

Fig. 12. HOL-packet arrival patterns within one frame. (a) Node's queue is nonempty. (b) Node's queue is empty.

Hence, the objective function $\sum_{n=2}^{N} f_n^2(\mathbf{a})$ is a nonnegative sum of convex functions $f_n^2(\mathbf{a})$ $(n = 2, 3, \ldots, N)$, which is also convex [30]. That is, the curve-fitting is a convex optimization problem.

Appendix B
Derivation of $E[W_{\rm st}]$ and $E[W_{\rm qt}]$

To calculate the average packet delay of the M/G/1 queue of a tagged node, we first derive the probability distribution of packet service time $W_{\rm st}$. For analysis simplicity, we normalize the control period of each frame as an integer multiple of one D-TDMA data slot duration T_p, i.e., $M = \lceil M_m T_m / T_p \rceil$, where $\lceil\ \rceil$ is the ceiling function. The end instant of each slot along one D-TDMA frame is numbered from 1 to $M + N$, as shown in Fig. 12. Let random variable J denote the arriving instant of each head-of-line (HOL) packet. It is assumed that HOL packets of the tagged node appear only at the end of each time slot, neglecting the possibility that HOL packets can arrive within the duration of each time slot [32], which means J takes discrete values from set $\mathbf{A} = \{1, 2, \ldots, M + N\}$. In Fig. 12, it can be seen that HOL packets have two different arriving patterns according to current status of the queue: 1) When the node's queue is nonempty (i.e., at least one packet staying in the queueing system), HOL packets can appear only at the end of its designated data slot in the data transmission period, which means J takes values from set $\mathbf{A}' = \{M + 1, M + 2, \ldots, M + N\}$; and 2) when the node's queue is empty (i.e., no packets are in service), HOL packets can arrive at any time instant in set $\mathbf{A}$. Next, we derive the distribution of $W_{\rm st}$ under these two cases.

When the node's queue is nonempty, based on the assumption that the data slot is randomly selected for each node in the next frame upon the successful packet transmission in the current frame, we use random variable I, which takes values from set $\mathbf{B} = \{1, 2, \ldots, N\}$, to denote the data slot number that the node selects in the next frame. Thus, the probability distribution of the packet service time $W_{\rm st}$ in the unit of one data slot duration, denoted by W_s, is derived as

$$\begin{aligned} &P\{W_s = M + k\} \\ &\quad = \sum_{j \in \mathbf{A}', i \in \mathbf{B}} P\{W_s = M + k, J = j, I = i\} \\ &\quad = \sum_{j \in \mathbf{A}', i \in \mathbf{B}} P\{W_s = M + k | J = j, I = i\} P\{J = j\} P\{I = i\} \\ &\quad = \frac{k}{N^2} \quad (1 \le k \le N) \\ &P\{W_s = M + N + k\} \\ &\quad = \frac{N - k}{N^2} \quad (1 \le k \le N - 1). \end{aligned} \tag{25}$$

When the node's queue is empty, HOL packets can arrive at any time instant in set $\mathbf{A}$. Thus, the probability distribution of W_s is derived in the following two cases.

1) If $M \ge N$m, then

$$\begin{aligned} P\{W_s = k\} &= \sum_{j=M-k+1}^{M-k+N} P\{W_s = k | J = j\} P\{J = j\} \\ &= \frac{1}{M + N} \quad (1 \le k \le N - 1) \\ P\{W_s = M - k\} &= \sum_{j=k+1}^{k+N} P\{W_s = M - k | J = j\} P\{J = j\} \\ &= \frac{1}{M + N}, \quad (0 \le k \le M - N) \\ P\{W_s = M + k\} &= \sum_{j=1}^{N-k} \sum_{j=M+N-k+1}^{M+N} P\{W_s = M + k | J = j\} \\ &\quad \cdot P\{J = j\} = \frac{1}{M + N}, \quad (1 \le k \le N). \end{aligned} \tag{26}$$

2) If $M < N$, then

$$\begin{aligned} P\{W_s = k\} &= \sum_{j=M-k+1}^{M-k+N} P\{W_s = k | J = j\} P\{J = j\} \\ &= \frac{1}{M + N}, \quad (1 \le k \le M) \\ P\{W_s = M + k\} &= \sum_{j=1}^{N-k} \sum_{j=M+N-k+1}^{M+N} P\{W_s = M + k | J = j\} \\ &\quad \cdot P\{J = j\} = \frac{1}{M + N}, \quad (1 \le k \le N). \end{aligned} \tag{27}$$

Hence, the average service time $E[W_{\rm st}]$ and the second moment of service time $E[W_{\rm st}^2]$ are derived as follows:

$$E[W_{\rm st}] = P_{\rm qn} \cdot \sum_{k_1 \in C} k_1 T_p P\{W_s = k_1\} + P_{\rm qe} \cdot \sum_{k_2 \in D} k_2 T_p P\{W_s = k_2\}$$
$$= \lambda E[W_{\rm st}] \cdot \sum_{k_1 \in C} k_1 T_p P\{W_s = k_1\} + (1 - \lambda E[W_{\rm st}]) \cdot \sum_{k_2 \in D} k_2 T_p P\{W_s = k_2\}$$
$$\Longrightarrow E[W_{\rm st}] = \frac{(M+N+1)T_p}{2 - \lambda(M+N-1)T_p} \tag{28}$$

$$E[W_{\rm st}^2] = \frac{(2M+2N+1)(M+N+1)T_p^2}{6} + T_p^2 \lambda E[W_{\rm st}] \cdot \left[(M+N)^2 + \frac{N^2-1}{6} - \frac{(2M+2N+1)(M+N+1)}{6} \right] \tag{29}$$

where $P_{\rm qe}$ is the queue empty probability, and $\mathbf{C}$ and $\mathbf{D}$ are two sets of possible values of W_s for the queue nonempty and queue empty cases, respectively.

REFERENCES

[1] M. Natkaniec, K. Kosek-Szott, S. Szott, and G. Bianchi, "A survey of medium access mechanisms for providing QoS in ad-hoc networks," *IEEE Commun. Survey Tuts.*, vol. 15, no. 2, pp. 592–620, 2nd Quart. 2013.

[2] P. Wang and W. Zhuang, "A collision-free MAC scheme for multimedia wireless mesh backbone," *IEEE Trans. Wireless Commun.*, vol. 8, no. 7, pp. 3577–3589, Jul. 2009.

[3] M. Natkaniec *et al.*, "Supporting QoS in integrated ad-hoc networks," *Wireless Pers. Commun.*, vol. 56, no. 2, pp. 183–206, Jan. 2011.

[4] G. Bianchi, "Performance analysis of the IEEE 802.11 distributed coordination function," *IEEE J. Sel. Areas Commun.*, vol. 18, no. 3, pp. 535–547, Mar. 2000.

[5] A. Kanzaki, T. Uemukai, T. Hara, and S. Nishio, "Dynamic TDMA slot assignment in ad hoc networks," in *Proc. IEEE AINA*, 2003, pp. 330–335.

[6] N. Wilson, R. Ganesh, K. Joseph, and D. Raychaudhuri, "Packet CDMA versus dynamic TDMA for multiple access in an integrated voice/data PCN," *IEEE J. Sel. Areas Commun.*, vol. 11, no. 6, pp. 870–884, Aug. 1993.

[7] W. Hu, X. Li, and H. Yousefi'zadeh, "LA-MAC: A load adaptive MAC protocol for MANETs," in *Proc. IEEE GLOBECOM*, 2009, pp. 1–6.

[8] R. Zhang, L. Cai, and J. Pan, "Performance study of hybrid MAC using soft reservation for wireless networks," in *Proc. IEEE ICC*, 2011, pp. 1–5.

[9] R. Zhang, L. Cai, and J. Pan, "Performance analysis of reservation and contention-based hybrid MAC for wireless networks," in *Proc. IEEE ICC*, 2010, pp. 1–5.

[10] R. Ahmed, "An adaptive multiple access protocol for broadcast channels," in *Proc. IEEE IPCCC*, 1997, pp. 371–377.

[11] I. Chlamtac, A. Farago, A. Myers, V. Syrotiuk, and G. Zaruba, "ADAPT: A dynamically self-adjusting media access control protocol for ad hoc-networks," in *Proc. IEEE GLOBECOM*, 1999, pp. 11–15.

[12] W. Hu, H. Yousefi'zadeh, and X. Li, "Load adaptive MAC: A hybrid MAC protocol for MIMO SDR MANETs," *IEEE Trans. Wireless Commun.*, vol. 10, no. 11, pp. 3924–3933, Nov. 2011.

[13] C. Doerr *et al.*, "MultiMAC-an adaptive MAC framework for dynamic radio networking," in *Proc. IEEE DySPAN*, 2005, pp. 548–555.

[14] D. Zheng and Y.-D. Yao, "Throughput performance evaluation of two-tier TDMA for sensor networks," in *Proc. IEEE SARNOFF*, 2009, pp. 1–5.

[15] L. Cai, X. Shen, J. W. Mark, L. Cai, and Y. Xiao, "Voice capacity analysis of WLAN with unbalanced traffic," *IEEE Trans. Veh. Technol.*, vol. 55, no. 3, pp. 752–761, May 2006.

[16] Z. Haas and J. Deng, "Dual busy tone multiple access (DBTMA)—A multiple access control scheme for ad hoc networks," *IEEE Trans. Commun.*, vol. 50, no. 6, pp. 975–985, Jun. 2002.

[17] L. Lei, S. Cai, C. Luo, W. Cai, and J. Zhou, "A dynamic TDMA-based MAC protocol with QoS guarantees for fully connected ad hoc networks," *Telecommun. Syst.*, vol. 60, no. 1, pp. 43–53, Sep. 2015.

[18] I. Chlamtac, M. Conti, and J. J.-N. Liu, "Mobile ad hoc networking: Imperatives and challenges," *Ad Hoc Netw.*, vol. 1, no. 1, pp. 13–64, Jul. 2003.

[19] H. Jiang, P. Wang, and W. Zhuang, "A distributed channel access scheme with guaranteed priority and enhanced fairness," *IEEE Trans. Wireless Commun.*, vol. 6, no. 6, pp. 2114–2125, Jun. 2007.

[20] A. Abdrabou and W. Zhuang, "Stochastic delay guarantees and statistical call admission control for IEEE 802.11 single-hop ad hoc networks," *IEEE Trans. Wireless Commun.*, vol. 7, no. 10, pp. 3972–3981, Oct. 2008.

[21] S. Jiang, J. Rao, D. He, X. Ling, and C. C. Ko, "A simple distributed PRMA for MANETs," *IEEE Trans. Veh. Technol.*, vol. 51, no. 2, pp. 293–305, Mar. 2002.

[22] K. Medepalli and F. Tobagi, "System centric and user centric queueing models for IEEE 802.11 based wireless LANs," in *Proc. IEEE BroadNets*, 2005, pp. 612–621.

[23] L. Kleinrock and F. Tobagi, "Packet switching in radio channels: Part I—carrier sense multiple-access modes and their throughput-delay characteristics," *IEEE Trans. Commun.*, vol. COMM-23, no. 12, pp. 1400–1416, Dec. 1975.

[24] A. Abdrabou and W. Zhuang, "Service time approximation in IEEE 802.11 single-hop ad hoc networks," *IEEE Trans. Wireless Commun.*, vol. 7, no. 1, pp. 305–313, Jan. 2008.

[25] G. Berger-Sabbatel, A. Duda, M. Heusse, and F. Rousseau, "Short-term fairness of 802.11 networks with several hosts," in *Proc. Mobile Wireless Commun. Netw.*, 2005, pp. 263–274.

[26] G. Berger-Sabbatel, A. Duda, O. Gaudoin, M. Heusse, and F. Rousseau, "Fairness and its impact on delay in 802.11 networks," in *Proc. IEEE GLOBECOM*, 2004, vol. 5, pp. 2967–2973.

[27] K. Medepalli and F. Tobagi, "Throughput analysis of IEEE 802.11 wireless LANs using an average cycle time approach," in *Proc. IEEE GLOBECOM*, 2005, vol. 5, pp. 3007–3011.

[28] Y. Tay and K. C. Chua, "A capacity analysis for the IEEE 802.11 MAC protocol," *Wireless Netw.*, vol. 7, no. 2, pp. 159–171, Mar./Apr. 2001.

[29] A. Kumar, E. Altman, D. Miorandi, and M. Goyal, "New insights from a fixed-point analysis of single cell IEEE 802.11 WLANs," *IEEE/ACM Trans. Netw.*, vol. 15, no. 3, pp. 588–601, Jun. 2007.

[30] S. P. Boyd and L. Vandenberghe,*Convex Optimization*. Cambridge, U.K.: Cambridge Univ. Press, 2004.

[31] M. Carvalho and J. Garcia-Luna-Aceves, "Delay analysis of IEEE 802.11 in single-hop networks," in *Proc. IEEE ICNP*, 2003, pp. 146–155.

[32] H. Omar, W. Zhuang, A. Abdrabou, and L. Li, "Performance evaluation of VeMAC supporting safety applications in vehicular networks," *IEEE Trans. Emerging Topics Comput.*, vol. 1, no. 1, pp. 69–83, Jun. 2013.

[33] D. P. Bertsekas, R. G. Gallager, and P. Humblet,*Data Networks*, vol. 2. Englewood Cliffs, NJ, USA: Prentice-Hall, 1987.

[34] [Online]. Available: http://www.omnetpp.org/omnetpp

[35] J. Ren *et al.*, "Lifetime and energy hole evolution analysis in data-gathering wireless sensor networks," *IEEE Trans. Ind. Informat.*, vol. 12, no. 2, pp. 780–800, Apr. 2016.

[36] *Supplement to IEEE Standard for Information Technology-Telecommunications and Information Exchange Between Systems-Local and Metropolitan Area Networks-Specific Requirements-Part 11: Wireless LAN Medium Access Control (MAC) and Physical Layer (PHY) Specifications: Higher-Speed Physical Layer Extension in the 2.4 GHz Band*, IEEE Std. 802.11b-1999, 2000, p. i-90.

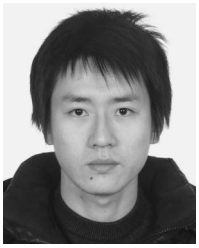

Qiang Ye (S'16) received the B.Sc. and M.Sc. degrees from Nanjing University of Posts and Telecommunications, Nanjing, China, in 2009 and 2012, respectively. He is currently working toward the Ph.D. degree with the Department of Electrical and Computer Engineering, University of Waterloo, Waterloo, ON, Canada.

His research interests include medium access control and performance optimization in mobile ad hoc networks.

Weihua Zhuang (M'93–SM'01–F'08) received the B.Sc. and M.Sc. degrees from Dalian Maritime University, Dalian, China, and the Ph.D. degree from the University of New Brunswick, Fredericton, NB, Canada, all in electrical engineering.

Since 1993, she has been with the Department of Electrical and Computer Engineering, University of Waterloo, Waterloo, ON, Canada, where she is currently a Professor and a Tier I Canada Research Chair in wireless communication networks. Her current research interests include resource allocation and quality-of-service provisioning in wireless networks, and smart grid.

Ms. Zhuang is an elected member of the Board of Governors and VP Mobile Radio of the IEEE Vehicular Technology Society. From 2008 to 2011, she was an IEEE Communications Society Distinguished Lecturer. In 2011, she served as the Technical Program Symposia Chair of the IEEE Global Communications Conference. From 2007 to 2013, she served as the Editor-in-Chief for the IEEE TRANSACTIONS ON VEHICULAR TECHNOLOGY. She coreceived several Best Paper Awards from IEEE conferences. In 2001, she received the Premiers Research Excellence Award from the Ontario Government and since 2005 has received the Outstanding Performance Award four times from the University of Waterloo. She is a Fellow of the Canadian Academy of Engineering and the Engineering Institute of Canada.

Li Li (M'03–SM'12) received the M.Sc. degree in electrical engineering from Southeast University, Nanjing, China, in 1990 and the Ph.D. degree in electrical engineering from the University of Ottawa, Ottawa, ON, Canada, in 1993.

From 1993 to 1999, she was with Nortel Networks Ltd. as a System Architect and then as a Product Manager. From 1999 to 2003, she was the Chief Architect at SS8 Networks Inc. Since 2003, she has been with the Communications Research Centre, Ottawa, ON, Canada, where she is currently a Senior Research Scientist. She has contributed previously to ITU-T and IETF standard working groups, coauthored IETF Request For Comments, and has been awarded several U.S. patents. She is the author of several papers presented and published in international conferences and journals, respectively. Her current research interests include spectrum-efficient wireless networking, adaptive networks, Internet of Things, data analytics, and decision-making algorithms.

Dr. Li served as a Cochair for the IEEE International Conference on Pervasive Computing and Communications Workshop on Mobile Peer-to-Peer Computing during 2006–2008, as a Track Cochair for the IEEE Vehicular Technology Conference in the Fall of 2010, as a session Cochair for the IEEE Military Communications Conference (MILCOM) during 2008–2014, and as a Track Cochair for MILCOM in 2012. From 2010 to 2013, she served as an Associated Editor for the *Springer Journal on Peer-to-Peer Networking and Applications* and for the IEEE TRANSACTIONS ON VEHICULAR TECHNOLOGY.

Philip Vigneron received the Ph.D. degree in electrical engineering from Queen's University, Kingston, ON, Canada, in 1999.

He is a Research Scientist and a Program Manager with the Communications Research Center, Ottawa, ON, Canada, which is a federal government research laboratory. His research interests include wireless communications, particularly modulation, coding, radio propagation, and robust waveform design for military applications, as well as topics supporting the development of wireless network connectivity on the battlefield. He has also been leading research programs in the area of fifth-generation wireless communications in the super high frequency bands and beyond.